A Truncated Floquet Wave Diffraction Method for the Full-Wave Analysis of Large Phased Arrays—Part II: Generalization to 3-D Cases

Andrea Neto, Stefano Maci, *Senior Member, IEEE*, Giuseppe Vecchi, *Member, IEEE*, and Marco Sabbadini

***Abstract*—This second part of a two-paper sequence deals with the generalization to three-dimensional (3-D) arrays of the truncated Floquet wave (TFW) diffraction method for the full wave analysis of large arrays. This generalization potentially includes arrays consisting of microstrip excited slots, cavity-backed apertures, and patches. The formulation is carried out first by deriving an appropriate fringe integral equation (IE) and next by defining entire domain basis functions in terms of global-array functions shaped as TFW diffracted rays whose analytical expression is derived on the basis of prototype canonical problems. The efficiency and the accuracy of this method is demonstrated by comparison with the results of an element-by-element full wave approach for a rectangular slot array.**

***Index Terms*—Electromagnetic diffraction, Floquet expansions, phased-array antennas.**

I. Introduction

In this paper, the truncated Floquet wave (TFW) full wave analysis proposed in [1] for two-dimensional (2-D) problems is extended to a quite large class of three-dimensional (3-D) finite-phased arrays. The assumption for applying this method is that the array exhibits a geometrical periodicity and is fed with a linear progressive phase. A simple example of such a linear-phase excitation is that produced by an incident plane wave; thus, the present method also includes actual scattering problems like those involving frequency selective surfaces (FSS). In the following, we will refer to radiating (antenna) problems keeping in mind that the analogy between antennas and plane wave scattering in our methodology is mainly confined to the assumption of the linear phase of the excitation. It is understood that most of the actual arrays are not perfectly periodic neither for the excitation nor for the geometry, but in many practical applications, the deviation with respect to the periodicity conditions is weak, thus allowing possible extensions of this method that will be here addressed.

The hypothesis of linear-phase excitation or, more generally, of periodic excitation, allows a very simple and efficient solution of the infinite array that is associated with the actual one in terms of Floquet wave (FW) expansions. These FW's are considered as producing diffraction effects and relevant fringe current perturbations at the edge of the array. The key point of the present procedure is to expand these fringe unknown currents in terms of diffracted rays and to find the unknown expansion (diffraction) coefficients by solving via method of moments a pertinent fringe integral equation (IE).

The type of array elements that can be studied with the present method include slots, cavity-backed apertures, dipoles in free-space, and patches. For this latter case, the formulation of the overall procedure is valid, but the explicit expressions of the basis functions we propose are applicable in practice only when the surface wave excitation is not significant; consequently, at the present state, the direct applicability of the present formulation for patch arrays is restricted to very low substrate dielectric constants, which are, however, widely employed in space applications.

This paper is organized as follows. Section II presents the generalization to three dimensional arrays of the truncated FW diffraction method introduced in Part I; this is carried out first by deriving a "fringe" IE and next by defining entire domain basis functions in terms of the FW diffracted rays. Section III presents the solution scheme for both the infinite array IE and the fringe IE. Explicit expressions for the ray-diffracted functions to be used in the solution scheme are presented in Section IV. Section V addresses the extension of this method to weak aperiodicity of both the array geometry and its excitation. The selection of the diffracted rays is discussed in Section VI on the basis of the results obtained in Part I; the numerical results are successfully compared with those from an element-by-element full wave solution for the case of a rectangular slot array. Finally, the basic features of the method are summarized in Section VII.

II. Formulation of the Integral Equations

Consider an array composed by N identical basic cells occupying regions S_i centered at the nodes $\vec{r}_i$ of a regular rectangular lattice in the x–y plane of a reference system. Fig. 1 refers to an array of patches just to illustrate the geometry for a practical case. Denote by d_x, d_y, and by $k_{xs}d_x$, $k_{ys}d_y$ the periodicity and the excitation phasings in the directions x and y, respectively. Inside each region S_i, A_i denotes the radiating surface on which we will apply the boundary (dipoles, patches) or continuity (slots, cavities) conditions. Note that each unit cell can contain more than one antenna element (two, for example, in Fig. 1) because the geometrical periodicity is not in general recovered element by element, e.g., for the presence of feeding lines, multiple polarized elements, etc. The total region occu-

Manuscript received October 6, 1997; revised January 7, 1999.

A. Neto and S. Maci are with the College of Engineering, University of Siena, Siena, 53100 Italy.

G. Vecchi is with the Department of Electronics, Politecnico di Torino, Corso Duca degli Abruzzi 24, Italy.

M. Sabbadini is with ESA-ESTEC, 2200 AG Noordwijk, The Netherlands.

Publisher Item Identifier S 0018-926X(00)02451-0.

pied by the array elements is denoted by $A = \cup_i A_i$ and it is contained in $\Sigma = \cup_i S_i$. Next, we introduce an infinite array, that coincides with the actual finite array on Σ and realizes the regular periodic continuation of the finite array on the region external to Σ, that we denote by Σ^* (Fig. 1). The two regions Σ and Σ^* are separated by the contour Γ. The portion of radiating surfaces of the infinite array contained in Σ^* will be denoted by A_i^* and $A^* = \cup_i A_i^*$.

The basic IE is formulated by use of the appropriate form of the equivalence theorem, which substitute the array by a distribution of equivalent electric or magnetic unknown sources $\vec{u}$ that radiate in an equivalent, simpler medium for which the Green's function is known in a convenient form (free-space, grounded half-space, or infinite layered dielectric media). The IE expresses the enforcement of the appropriate boundary conditions on the actual surface A (vanishing of tangential electric field on conductors or continuity of magnetic field through apertures) for the total field (impressed plus radiated by equivalent currents). Since these conditions have to be enforced on the radiators of the array only, it is convenient to express the fields in terms of the characteristic function of the various regions of interest; for a generic region B, this function will be denoted by χ_B, with $\chi_B(\vec{r}) = 1$ for $\vec{r} \in B$ and zero outside B. The general form of the $\mathbb{E}$ for the finite array can be compactly expressed as

$$\chi_A \vec{\mathcal{G}}[\vec{u}] = \chi_A \vec{v}_f \tag{1}$$

where

- χ_A characteristic function of the surface A of the finite array;
- $\vec{\mathcal{G}}[\vec{u}]$ field produced by the equivalent source $\vec{u}$ in the equivalent medium;
- $\vec{v}_f$ forcing field that represents the array excitation.

For instance, in case of apertures in ground planes, $\vec{u}$ is the magnetic current and $\vec{v}_f$ is the driving magnetic field on the shorted apertures, respectively, and the kernel of the integral operator $\vec{\mathcal{G}}[\vec{u}]$ is the (magnetic) dyadic Green's function for the shorted half-space. Conversely, in a patch/dipole problem, $\vec{u}$ and $\vec{v}_f$ are the electric current and tangential forcing field on the removed conductors, respectively, and the kernel of $\vec{\mathcal{G}}[\vec{u}]$ is the (electric) dyadic Green's function for the free-space or the layered dielectric. We remark that in the case of apertures opening onto waveguides or over printed circuits, the construction of the term $\vec{\mathcal{G}}[\vec{u}]$ may be consistently complex, however, we stress that the relevant issue dealt with here refers to the *external* interactions at array level; this latter aspect will remain unaffected by a more complicated problem with interior–exterior coupling properties. According to the formulation for the 2-D case developed in [1], we now write the solution $\vec{u}$ as

$$\vec{u} = \chi_A \vec{u}_\infty + \vec{u}_d, \qquad \text{with } \vec{u}_d = \vec{u} - \chi_A \vec{u}_\infty \tag{2}$$

where $\vec{u}_\infty$ is the solution of the infinite array problem

$$\chi_\infty \vec{\mathcal{G}}[\vec{u}_\infty] = \chi_\infty \vec{v}_f \tag{3}$$

and $\chi_\infty = \chi_{A+A^*} = \chi_A + \chi_{A^*}$ is the characteristic function of the infinite array.

We observe that $\chi_\infty \vec{\mathcal{G}}[\vec{u}_\infty] - \chi_\infty \vec{v}_f = 0$ must hold everywhere in the surface occupied by the infinite array and, thus, (3) is unchanged by multiplication by χ_A; therefore, inserting (2) into (1), and making use of (3), the original problem transforms into

$$\chi_A \vec{\mathcal{G}}[\vec{u}_d] = \chi_A \vec{v}_{\text{ext}} \tag{4}$$

$$\vec{v}_{\text{ext}} = \vec{\mathcal{G}}[\chi_{A^*} \vec{u}_\infty]. \tag{5}$$

This latter is the generalized fringe IE that represents the same boundary conditions as the original IE (1), but with a different forcing term, which is produced by the sources $\vec{u}_{\text{ext}} = \chi_{A^*} \vec{u}_\infty$ external to Σ. Therefore, $\vec{u}_d$ is the field on the actual radiators of the finite array produced by the sources $\vec{u}_{\text{ext}}$ in the presence of the real array. The forcing term $\vec{v}_{\text{ext}}$ of (4) is the field radiated in the equivalent medium by that part of the infinite array which has been suppressed to obtain the actual problem from the infinite one and expresses the deformation of the finite-array solution u_d as the term that is necessary to compensate the absence of the radiation contribution from the array suppressed part $(\vec{u}_{\text{ext}})$.

Although the above interpretation of $\vec{v}_{\text{ext}}$ clarifies the physical meaning of the fringe IE, it may be interesting to express the forcing term in (4) as independent of the definition of the external part of the array. To this end, we let $\vec{u}_{\text{int}} = \chi_\Sigma \vec{u}_\infty$ so that (5) becomes $\vec{v}_{\text{ext}} = -(\vec{v}_{\text{int}} - \vec{v}_\infty)$, where $\vec{v}_\infty = \vec{\mathcal{G}}[\vec{u}_\infty]$ and $\vec{v}_{\text{int}} = \vec{\mathcal{G}}[\vec{u}_{\text{int}}]$. Note that $\vec{v}_{\text{int}}$ is exactly the same as that obtained from the usual windowing approach; this allows us to attribute to the quantity $(\vec{v}_{\text{int}} - \vec{v}_\infty) = \vec{v}_d^{\,\text{PO}}$ the meaning of diffracted field from the truncated FW's generated by $\vec{u}_{\text{int}}$. The superscript PO reminds one that this diffracted field is calculated from the

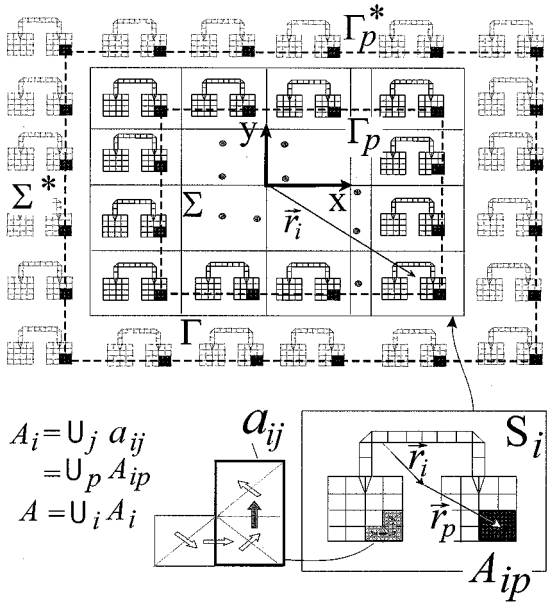

Fig. 1. Example of complex large finite array and relevant geometry. The regions S_i denotes the periodicity cell of the array. The regions a_{ij} are the supports of the subdomain basis functions (i.e., rooftop) employed to discretize the structure in the MoM analysis of the single cell S_i in the infinite array. The regions A_{ip} group a certain number of a_{ij} and represent collectively the support of the array $C_p(\vec{r}\,)$, which is globally visualized by the black cells inside the boundary Γ_p. The support of the array $C_p^*(\vec{r}\,)$ is visualized by the black cells external to Γ_p^*.

unperturbed abruptly truncated sources, as in the physical optics (windowing) approach. Consequently, (4) is rewritten as

$$\chi_A \vec{\mathcal{G}}[\vec{u}_d] = -\chi_A \vec{v}_d^{\,\mathrm{PO}}. \tag{6}$$

This IE is perfectly equivalent to (4), since no approximations have been made. However, its direct use in the method of moments (MoM) solution scheme may be sometimes convenient for the reasons that we will discuss in the last section.

III. Solution Scheme

In this section, the solution scheme of the IE's (3) and (4) will be presented. Since the solution of the infinite array problem (3) is well known, it is just summarized in order to set suitable notations.

A. Solution of the Infinite-Array Integral Equation

Equation (3) represents the IE for the infinite periodic array. As is well known, the hypothesis of periodicity of geometry and excitation allows the reduction of the problem to that of a single periodic basic cell. This cell is placed inside an infinite waveguide with cross section S_i orthogonal to the array plane, and with phase-shift conditions on the walls to reproduce the phasing of the image sources. The formulation may be carried out by using an ordinary MoM scheme, with basis functions $\vec{f}_j(\vec{r}-\vec{r}_i)$; $j=1,\cdots,J$ defined on small, overlapped subdomains a_{ji}, which collectively cover the domain $A_i=\cup_j a_{ji}$ (e.g., roof-top, see Fig. 1). The final solution can be expressed by

$$\vec{u}_\infty(\vec{r}) = \sum_{i=-\infty}^{\infty} \vec{u}_{0\infty}(\vec{r}-\vec{r}_i)e^{-j\vec{k}_s\cdot\vec{r}_i} \tag{7}$$

where $\vec{k}_s = k_{xs}\hat{x} + k_{ys}\hat{y}$ and

$$\vec{u}_{0\infty}(\vec{r}) = \chi_{A_0} \sum_{j=1}^{J} \vec{f}_j(\vec{r}) U_{j\infty} \tag{8}$$

is the solution for the single cell A_0, placed for convenience at $\vec{r}_i = 0$. The above formulas are also valid when using entire domain basis functions defined over A_i as more convenient for slots or open ended cavities.

B. Solution of the Fringe Integral Equation

In principle, the size of the subcells a_{ji} in the solution of the infinite array is a function of the operating wavelength; in practice, however, for radiators of resonant size (like patches or apertures), the mesh has to be much finer than necessary for correctly representing a smooth wavefunction, and instead the mesh subcell size is dictated by the field discontinuities at edges, corners, feed points, etc. As a result, the subcell size is essentially the same as that necessary for solving a static problem for that geometry and, thus, almost independent of the frequency. It is important to note that these quasi-static, near-field effects are essentially the same for the actual array and for the basic cell of the infinite periodic array. As a result, the behavior at various discontinuities and edges is already accounted for by the solution of the infinite array $\vec{u}_\infty(\vec{r})$; instead, as clear from the fringe formulation (4), the difference term $\vec{u}_d$ is dominated by wave phenomena, i.e., by dynamic, as opposed to quasi-static, effects. As a result, our formulation has the advantage of allowing for a relaxation of the mesh size both when solving for $\vec{u}_d$ and when calculating $\vec{v}_{\mathrm{ext}}$: we therefore employ now a different, coarser mesh. To this purpose let us divide every region $A_i(A_i^*)$ into P subdomain regions $A_{pi}(A_{pi}^*)$ centered at $\vec{r}_{pi}=\vec{r}_p+\vec{r}_i$ (Fig. 1) where for convenience assume $\vec{r}_i=0$ for $i=0$. Note that A_{pi} includes a certain number N_p of a_{ji}. On each A_{pi}, we define basis functions $\vec{c}_p(\vec{r}-\vec{r}_{pi})$, which are zero outside A_{pi}, and collect N_p subdomain basis functions $\vec{f}_j$ weighted with the coefficient of the infinite array solution; i.e.,

$$\vec{c}_p(\vec{r}-\vec{r}_{pi}) = \chi_{A_{pi}} \sum_{j=1}^{N_p} \vec{f}_j(\vec{r}-\vec{r}_i) U_{j\infty}. \tag{9}$$

These basis functions are used in the representation of the forcing term $\vec{v}_{\mathrm{ext}}(\vec{r})$ as described next.

1) Diffracted Ray Representation of the Forcing Term: It is convenient to start from the representation of $\vec{v}_{\mathrm{ext}}(\vec{r})$ because it gives a guideline for that of $\vec{u}^d(\vec{r})$. To this end, let us define an infinite phased array of sources

$$\vec{C}_{p\infty}(\vec{r}) = \sum_{i=-\infty}^{\infty} \vec{c}_p(\vec{r}-\vec{r}_{pi})e^{-j\vec{k}_s\cdot\vec{r}_i} \tag{10}$$

which has the same periodicity and excitation as the original array, but unlike the latter, is composed of a collection of relatively small domain elements whose p-summation exactly reconstructs the infinite array. The field radiated by $\vec{C}_{p\infty}(\vec{r})$, namely $\vec{v}_{p\infty}(\vec{r}) = \vec{\mathcal{G}}(\vec{C}_{p\infty}(\vec{r}))$, can be represented in terms of the FW expansion

$$\vec{v}_{p\infty}(\vec{r}) = \sum_{m=-\infty}^{\infty} \vec{V}_{mp\infty} e^{-j\vec{k}_m\cdot\vec{r}} \tag{11}$$

where $\vec{r}$ is an arbitrary observation point on the array plane (x, y), m denotes the double index (m_x, m_y) and

$$\begin{aligned} \vec{k}_m &= k_{xm_x}\hat{x} + k_{ym_y}\hat{y} + k_{zm_xm_y}\hat{z} \\ & m_x, m_y = 0, \pm 1, \pm 2, \cdots \end{aligned} \tag{12}$$

where

$$\begin{aligned} k_{xm_x} &= k_{xs} + \frac{2\pi m_x}{d_x}, \quad k_{ym_y} = k_{ys} + \frac{2\pi m_y}{d_y} \\ k_{zm_xm_y} &= \sqrt{k^2 - k_{xm_x}^2 - k_{ym_y}^2} \end{aligned} \tag{13}$$

are the propagation constants in the array plane direction of the mth FW with explicit dependence on the beam-scanning phase shift (k_{xs}, k_{ys}) imposed by the beam forming network.

Also, define the phased arrays $\vec{C}_p(\vec{r})$ and $\vec{C}_p^*(\vec{r})$ as the portions of $\vec{C}_{p\infty}(\vec{r})$ having support in A and A^*, respectively, i.e.,

$$\vec{C}_p(\vec{r}) = \chi_A \vec{C}_{p\infty}(\vec{r}), \qquad \vec{C}_p^*(\vec{r}) = \chi_{A^*} \vec{C}_{p\infty}(\vec{r}). \tag{14}$$

Denote by Γ_p and Γ_p^* the rectangular boundary contours of $\vec{C}_p$ and $\vec{C}_p^*$, respectively; they pass through the phase centers of the boundary elements of $\vec{C}_p(\vec{r})$ and $\vec{C}_p^*(\vec{r})$, respectively

(Fig. 1). Since the p-summation of $\vec{C}_p^*$ constructs the external array $\vec{u}_{\text{ext}} = \chi_{A^*}\vec{u}_\infty$, the forcing term in (4) is represented as

$$\vec{v}_{\text{ext}}(\vec{r}) = \sum_{p=1}^{P} \vec{v}_{ext,\,p}(\vec{r}) \tag{15}$$

where

$$\vec{v}_{ext,\,p}(\vec{r}) = \vec{\mathcal{G}}\left(\vec{C}_p^*(\vec{r})\right) \tag{16}$$

is the field contribution radiated on A by the array $\vec{C}_p^*(\vec{r})$. As discussed in Part I of this paper, the physical mechanism that leads to the representation of $\vec{v}_{ext,\,p}$, can be described in terms of diffracted rays that each FW in (11) excites at Γ_p^*, i.e.,

$$\vec{v}_{ext,\,p}(\vec{r}) \sim \sum_q \sum_m \vec{v}_{mqp}(\vec{r}); \qquad \vec{r} \in A \tag{17}$$

where $\vec{v}_{mqp}(\vec{r})$ are the normalized qth diffracted ray-fields excited at Γ_p^* by the mth FW of $\vec{C}_{p\infty}(\vec{r})$. These rays are depicted in Fig. 2, and their explicit expression will be given in Section IV.

2) Representation of the Unknown Current: Extending the criterion introduced in [1], a diffracted ray expansion is also adopted for the unknown $\vec{u}_d(\vec{r})$, which is assumed to have a diffractive nature like that of $\vec{v}_{\text{ext}}(\vec{r})$. To this end a convenient choice for the MoM representation of $\vec{u}_d(\vec{r})$ are the entire domain basis functions

$$\vec{B}_{mq}(\vec{r}) = \vec{B}^0(\vec{r}) a_{mq}(\vec{r}) \tag{18}$$

obtained by modulating the array function

$$\vec{B}^0(\vec{r}) = \sum_{p=1}^{P} \vec{C}_p(\vec{r}) = \chi_A \sum_i \vec{u}_{0\infty}(\vec{r} - \vec{r}_i)$$

with the diffracted-ray functions $a_{mq}(\vec{r})$, whose explicit expressions are given in the next section [Section IV (27), (32)]. The unknown function $\vec{u}_d(\vec{r})$ will be then represented by

$$\vec{u}_d(\vec{r}) = \sum_q \sum_m U_{mq}\vec{B}_{mq}(\vec{r}) \tag{19}$$

and the unknown coefficient U_{mqp} will be obtained by application of the MoM procedure to the fringe IE. Note that the expression of $\vec{u}_d(\vec{r})$ respects the edge conditions on the individual element, because of the simple amplitude modulation we have assumed. In (18), the shape of the fringe unknown currents remains the same as that for the infinite array, except for the diffracted-like modulation $a_{mq}(\vec{r})$. This assumption has been found adequate for resonant element, and it is under investigation for nonresonant element like open-ended waveguide antenna elements. On the other hand, if one views the infinite array current distribution as zeroth-order approximation, then the diffracted currents associated to different element-distribution shape would represent only a second-order correction. Preliminary results on nonresonant element have shown that this second-order correction may be nonnegligible in describing cross-polar component in wide-beam scanning.

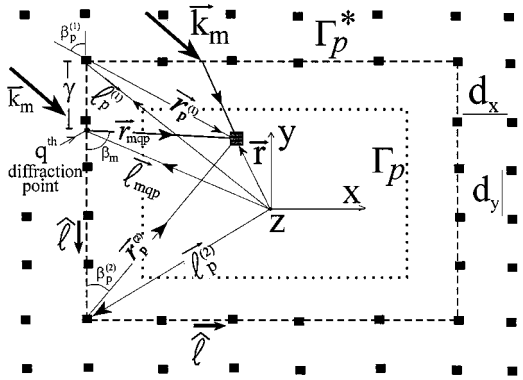

Fig. 2. Diffracted ray contributions in a given point $\vec{r}$ internal to Γ_p, excited by a Γ_p^*-truncated FW. The FW propagates with wavenumber $\vec{k}_m$. The diffracted rays arise from the verteces and from points q on the edges of Γ_p^*.

C. Construction of the Linear System

The conventional MoM solution is now obtained projecting (4) onto appropriate weight functions $\vec{W}_{mqp}(\vec{r})$, which yields the linear system

$$\sum_j U_j G_{ij} = F_i; \qquad i = mq,\; j = m'q' \tag{20}$$

where

$$G_{ij} = \left\langle \vec{W}_i(\vec{r}),\; \vec{\mathcal{G}}\left[\vec{B}_j(\vec{r})\right] \right\rangle_A,$$
$$F_i = \left\langle \vec{W}_i(\vec{r}),\; \vec{v}_{\text{ext}} \right\rangle_A \tag{21}$$

and the inner product $\langle \cdot,\, \cdot \rangle_A$ is the usual reaction-type integral on A.

The number of ray-type basis function $a_{mq}(\vec{r})$ sufficient to ensure an accurate solution is quite small and essentially independent of the global size of the array; thus, resulting in a linear system whose dimension is extremely small as compared to that of a conventional element-by-element solution. In most practical cases the only diffracted ray functions to be included are those associated with the propagating FW's plus one evanescent FW, this latter different for each edge. This was verified in the 2-D case of [1] and will be discussed later on with the aid of practical 3-D examples.

IV. TFW Diffracted Rays

A key point of this method is the suitable description of the TFW diffracted rays, namely of the ray-functions $\vec{v}_{mqp}(\vec{r})$ and $a_{mq}(\vec{r})$. To this end, we note that selecting basis functions $\vec{c}_p$ with relatively small domains allows the approximation of the array $\vec{C}_p^*$ in (10) with an array of elementary electric or magnetic dipoles located at the phase center of A_{pi}

$$\vec{C}_p^*(\vec{r}) \cong \chi_{A^*} \sum_i \vec{I}_p \delta(\vec{r} - \vec{r}_{pi}) e^{-j\vec{k}_s \cdot \vec{r}_i} \tag{22}$$

where $\vec{I}_p$ is the moment of the employed current on the subcell

$$\vec{I}_p = \iint_{A_{p0}} \vec{c}_p(\vec{r} - \vec{r}_{p0})\, dx\, dy. \tag{23}$$

This allows the approximation of the term $\vec{v}_{ext,p}$ with the active Green's function of a rectangular array of elementary dipoles. Next, by invoking the locality of the high-frequency phenomena as formalized in the geometrical theory of diffraction (GTD), the asymptotic diffracted rays of C_p^* can be calculated by the Green's functions of canonical arrays that locally fit the actual geometry of C_p^*, like a semi-infinite array of dipoles [2], [3] (for edge-diffracted rays), or a corner of dipoles [4] (for vertex rays). The formulation presented herein after can be derived from [2]–[4] by algebraic manipulations which lead to expressions in ray-fixed reference systems.

A. Edge Diffracted Rays

Consider first one finite side of the rectangular contour Γ_p^* whose length L is delimited by the two vertex points $\vec{\ell}_p^{(1)}$ and $\vec{\ell}_p^{(2)}$ (Fig. 2). We denote by $\hat{\ell}$ the unit vector along $\vec{\ell}_p^{(1)} - \vec{\ell}_p^{(2)}$, which is parallel to the side L to which the qth diffraction point belongs; hence, $\hat{\ell} = \hat{\ell}(q)$ and on the four sides of this rectangular contour $\hat{\ell}(q)$ is identified by $-\hat{x}$, $-\hat{y}$, $\hat{x}$, $\hat{y}$. For a given observation point $\vec{r}$, the qth ray diffracted at the side L and associated with the mth FW of $\vec{C}_{p\infty}$ in (10) and (11), propagates along a ray direction $\hat{r}_{mq}$ according to the generalized Fermat principle for TFW diffracted rays [3]

$$k\hat{r}_{mq} \cdot \hat{\ell} = \vec{k}_m \cdot \hat{\ell} = k \cos \beta_m. \tag{24a}$$

Equation (24a) establishes uniquely the diffraction point position vector $\vec{\ell}_{mqp}$ in analytical form as

$$\begin{aligned} \vec{\ell}_{mqp} &= \vec{\ell}_p^{(1)} + \gamma\hat{\ell}; \\ \gamma &= \vec{r}_p^{(1)} \cdot \hat{\ell} - \left|\vec{r}_p^{(1)} - \vec{r}_p^{(1)} \cdot \hat{\ell}\hat{\ell}\right| \cot \beta_m \end{aligned} \tag{24b}$$

where $\vec{r}_p^{(1)} = \vec{r} - \vec{\ell}_p^{(1)}$ is the observation point from vertex 1. Note that for the present case of rectangular contour, no numerical minimization of a distance function is needed for the ray tracing. From [2] and [3], one has

$$\begin{aligned} \vec{v}_{mpq}(\vec{r}) = {} & V_m^{(\mathrm{I})} \alpha_{mpq}^{(\mathrm{I})}(\vec{r}) \hat{t}_{mq} \hat{t}_{mq} \cdot \vec{I}_p \\ & + V_m^{(\mathrm{II})} \alpha_{mpq}^{(\mathrm{II})}(\vec{r}) \left(\vec{I}_p - \frac{1}{k^2} \vec{k}'_m \vec{k}'_m \cdot \vec{I}_p \right) \end{aligned} \tag{25}$$

where $\hat{t}_{mq} = \hat{z} \times \hat{r}_{mq}$ is the vector transverse to the diffracted ray direction and $\vec{k}'_m = -\hat{z} \times (\hat{z} \times \vec{k}_m)$ is the component of the FW propagating vector on the array plane. Furthermore

$$\alpha_{mpq}^{(\mathrm{I})}(\vec{r}) = [\eta(\gamma) - \eta(\gamma - L)] e^{-j\vec{k}_m \cdot \vec{\ell}_{mpq}} \frac{e^{-jkr_{mqp}}}{(kr_{mqp})^{1/2}} \tag{26}$$

and

$$\begin{aligned} \alpha_{mpq}^{(\mathrm{II})}(\vec{r}) = {} & [\eta(\gamma) - \eta(\gamma - L)] e^{-j\vec{k}_m \cdot \vec{\ell}_{mpq}} \\ & \cdot \frac{e^{-jkr_{mqp}}}{(\delta_m r_{mqp})^{3/2}} \mathcal{F}_s(\delta_m r_{mqp}) \end{aligned} \tag{27}$$

where

$$r_{mqp} = \left| \vec{r} - \vec{\ell}_{mqp} \right| \tag{28}$$

and

$$\delta_m = \left[k \sin \beta_m + \vec{k}_m \cdot (\hat{\ell} \times \hat{z}) \right] \sin \beta_m. \tag{29}$$

In (27)–(29), $\hat{z}$ is the normal to the array and $\mathcal{F}_s$ is the UTD slope transition function defined in [1, eq. (18)]. The expression of the coefficients $V_m^{(\mathrm{I})}$ and $V_m^{(\mathrm{II})}$ in (25) are

$$V_m^{(\mathrm{I})} = \frac{-\zeta k \sqrt{2\pi j}/(4\pi d_A \sin \beta_m)}{1 - \exp[-jd_B(k \sin \beta_m + \vec{k}_s \cdot (\hat{\ell} \times \hat{z})]} \tag{30}$$

$$V_m^{(\mathrm{II})} = \frac{-\zeta k \sqrt{2\pi j}}{4\pi\, d_x\, d_y \sqrt{k^2 - |\vec{k}_m \times \hat{z}|^2}} \tag{31}$$

where ζ is the characteristic free-space impedance or admittance depending on whether $\vec{v}_{mpq}$ represents an electric field (radiated by an electric dipole array) or a magnetic field (radiated by a magnetic dipole array), respectively. In (30), (d_A, d_B) denote (d_x, d_y) for $\hat{\ell} = \pm\hat{x}$ and (d_y, d_x) for $\hat{\ell} = \pm\hat{y}$. Equation (27) also defines the diffracted ray functions $a_{mq}(\vec{r})$ in (18) as

$$a_{mq}(\vec{r}) = \sum_{p=1}^{P} \alpha_{mpq}^{(\mathrm{II})}(\vec{r}). \tag{32}$$

It is important to remark on the following points.

1) Since the observation point $\vec{r}$ is *always on* A and the diffraction points occur on Γ_p^*, r_{mqp} is always large enough to justify the accuracy of the second-order asymptotic expansion in (25).
2) The asymptotic construction in (25) contains a dominant $(kr_{mqp})^{-1/2}$ ray-field contribution transverse to the ray direction $\hat{r}_{mq}$ and a second-order field contribution of order $(kr_{mqp})^{-3/2}$, which possesses components along both $\hat{r}_{mq}$ and $\hat{t}_{mq}$. This latter contains a transition function $\mathcal{F}_s(\delta_m r_{mqp})$ which is unity except when δ_m tends to vanish, which occurs when the mth FW is close to its cutoff. In this case, the transition function provides a modification of the ray-spreading factor so that its associated contribution becomes dominant.
3) The leading asymptotic contribution $V_m^{(\mathrm{I})} \alpha_{mpq}^{(\mathrm{I})}(\vec{r})$ in (25) is produced by the summation of all those FW's having the same k-vector projection along $\hat{\ell}$, namely to all those FW's whose diffraction occurs at the same edge point Q.
4) The diffracted ray basis functions $a_{mq}(\vec{r})$ that modulate the array function $\vec{B}_0$ in (18) are calculated by summation of the p-contribution of the second order ray functions $\alpha_{mpq}^{(\mathrm{II})}(\vec{r})$ generated by $\vec{C}_p$, this latter being the same as that rigorously found for the excitation term $\vec{v}_{mqp}(\vec{r})$. Retaining only the second-order contribution in the modulating function is what we suggested and motivated in [1] with reference to the 2-D case. The validity of this choice in this 3-D case will be confirmed by the results presented next.
5) The number of diffracted rays $\vec{v}_{mpq}$ required for an accurate estimate of $\vec{v}_{ext,p}(\vec{r})$ is not necessarily equal to the number of ray-functions $\alpha_{mpq}^{(\mathrm{II})}(\vec{r})$ required for the description of the p-type unknown. This latter number may be significantly lower, as will be discussed in Section V.

6) The Heaviside unit step functions $\eta(\gamma)$ in (26) and (27) force the ray contribution to vanish when the diffraction point slides out from one vertex, thus creating a jump discontinuity in the field definition. This jump can be compensated by adding vertex diffracted rays as suggested next.

B. Vertex Diffracted Rays

The edge diffracted ray function may be refined by adding two vertex diffracted rays that provide a uniform continuity of the total field when the diffraction point disappears from the truncated edge ($\gamma = 0, L$). To this end, the modified expressions

$$\underset{\sim}{\vec{v}}_{mpq}(\vec{r}) = \vec{v}_{mpq}(\vec{r}) + \vec{v}^{(1)}_{mp}(\vec{r}) + \vec{v}^{(2)}_{mp}(\vec{r}) \tag{33}$$

can be used in place of (25), where

$$\begin{aligned}\vec{v}^{(1)}_{mp}(\vec{r}) =& V^{(\mathrm{I})}_m \alpha^{(\mathrm{I},1)}_{mp}(\vec{r}) \hat{t}^{(1)}_p \hat{t}^{(1)}_p \cdot \vec{I}_p \\ &+ V^{(\mathrm{II})}_m \alpha^{(\mathrm{II},1)}_{mp}(\vec{r}) \left(\vec{I}_p - \frac{1}{k^2} \vec{k}'_m \vec{k}'_m \cdot \vec{I}_p \right)\end{aligned} \tag{34}$$

in which

$$\alpha^{(\mathrm{I},1)}_{mp}(\vec{r}) = \frac{e^{-jkr^{(1)}_p}}{kr^{(1)}_p} e^{-j\vec{k}_m \cdot \vec{\ell}^{(1)}_p} \frac{\sin\beta^{(1)}_p \mathcal{F}\left(r_{mqp}\mu^{(1)}_{mqp}\right)}{\sqrt{2\pi j}\left(\cos\beta_m - \cos\beta^{(1)}_p\right)} \tag{35}$$

$$\begin{aligned}\alpha^{(\mathrm{II},1)}_{mp}(\vec{r}) =& \frac{e^{-jkr^{(1)}_p}}{\left(\delta_m r^{(1)}_p\right)^2} e^{-j\vec{k}_m \cdot \vec{\ell}^{(1)}_p} \mathcal{F}_s(\delta_m r_{mqp}) \\ &\cdot \frac{\sqrt{\delta_m}\sin\beta^{(1)}_p \mathcal{F}\left(r^{(1)}_p \mu^{(1)}_{mqp}\right)}{\sqrt{2\pi jk}\left(\cos\beta_m - \cos\beta^{(1)}_p\right)}.\end{aligned} \tag{36}$$

In (35) and (36), $\vec{r}^{(1)}_p$ is the observation point from the vertex 1 with $\hat{r}^{(1)}_p$ its relevant unit vector and

$$\cos\beta^{(1)}_p = \hat{r}^{(1)}_p \cdot \hat{\ell} \tag{37}$$

$$\hat{t}^{(1)}_p = \hat{z} \times \hat{r}^{(1)}_p. \tag{38}$$

Furthermore, $\mathcal{F}$ is the UTD transition function defined in [1, eq. (18)] whose argument

$$\begin{aligned}r^{(1)}_p \mu^{(1)}_{mqp} =& k\left(r^{(1)}_p - r_{mqp}\right) - \gamma \vec{k}_m \cdot \hat{\ell} \\ =& 2kr^{(1)}_p \sin^2\left(\tfrac{1}{2}\left(\beta^{(1)}_p - \beta_m\right)\right)\end{aligned} \tag{39}$$

is the difference between the phases of the vertex and that of the edge diffracted rays. The expression of the contribution $\vec{v}^{(2)}_{mp}(\vec{r})$ from the vertex at $\hat{\ell}^{(2)}_p$ is obtained by the formal substitution $1 \rightarrow 2$ and $\hat{\ell} \rightarrow -\hat{\ell}$. The basis functions for the representation of the unknown will be obtained by using in (32) the modified expressions

$$\underset{\sim}{a}_{mq}(\vec{r}) = \sum_{p=1}^{P} \left(\alpha^{(\mathrm{II})}_{mpq}(\vec{r}) + \alpha^{(\mathrm{II},1)}_{mp}(\vec{r}) + \alpha^{(\mathrm{II},2)}_{mp}(\vec{r}) \right). \tag{40}$$

Note that the use of the above expression in the MoM solution of the fringe IE does not augment the number of unknowns. For a detailed explanation of the uniform compensation mechanisms provided by the vertex diffraction ray fields, one may refer to [5], which is relevant to the plane scattering at a perfectly conducting plane angular sector. Note that the vertex contributions $\vec{v}^{(1)}_{mp}$ and $u^{(1)}_{mp}$ are of higher asymptotic order with respect to $\vec{v}_{mpq}$ and u_{mpq}, respectively, except when $\mu^{(1)}_{mqp} = 0$ ($\gamma = 0$), where they become of the same asymptotic order as the edge contributions and provide continuity to the total field.

C. Layered Structures

Before proceeding further, we note that the representation in (17) with the definition (25) or (33) is incomplete when dealing with layered structures (patch arrays). Indeed, when a FW impinges on Γ^*_p, the diffracted field also excites guided waves inside the dielectric, [i.e., surface waves (SW's) and leaky waves (LW's)] [6]–[8]. While these latter may be neglected on A as they are exponentially attenuated away from Γ^*_p, the inclusion of SW's-shaped basis functions into the ray-field expansion (25) and (33) is important, especially for high thickness/permittivity. The SW-shaped basis functions have a unit spreading factor and propagate along a direction which is dictated by $\vec{k}_m$, again in accordance with a generalized Fermat principle (see [8, fig. 4, eq.(33)]), which can be solved in analytical form provided that the phase velocity of SW's (i.e., the SW poles of the pertinent spectral Green's function) is known. Furthermore, the presence of these waves imposes additional edge-diffracted rays which are significant close to the transition of SW's at cut-off, and additional vertex-diffracted rays to compensate for the shadow boundary line of the SW's on Σ. Since the complete discussion and the pertinent formulation on this subject would be too long, this particular issue will be treated elsewhere. However, the present formulation can be applied in the present form for patch arrays on very low substrate dielectric constants, which are of practical use for space applications.

V. Nonuniformity of Excitation and Periodicity

The physical interpretation attributed to the IE (4) has an apparent practical consistency only for the case when the array is periodic and periodically excited, because only for this case it is strictly possible to define $\vec{u}_\infty$ and its FW field expansion. For actual phased-array antennas, the global phase tapering of the array excitation is typically periodic, but the global amplitude does not necessarily need to be so. Furthermore, for traveling-wave arrays the basic cell is sometimes gradually modified to compensate for the leakage of the feeding wave. For these cases the present procedure may be applied taking into account the following considerations.

A. Smooth Tapering of the Array Excitation

When a smooth tapering $T(\vec{r})$ of the excitation occurs over the entire domain Σ of the array, the present procedure may be applied as well by invoking the local nature of the high-frequency (HF) phenomena. In particular, a local infinite array can be defined for each cell as the periodic continuation of the investigated basic cell with its local amplitude excitation. This is

equivalent to adiabatically modifying the infinite array solution as

$$\vec{u}_{\infty}^{T}(\vec{r}) = T(\vec{r})\vec{u}_{\infty}(\vec{r}) \tag{41}$$

which strictly resembles the familiar asymptotic definition of the PO currents in terms of the local incident field. As a result, in solving the fringe IE, the basic array of sources $\vec{C}_{p\infty}(\vec{r})$ in (10) is replaced by $T(\vec{r})\vec{C}_{p\infty}(\vec{r})$, thus producing a $T(\vec{r})$-amplitude modulation of each relevant FW. Note that the above operation requires the analytical continuation of the function $T(\vec{r})$ in the external region Σ^*. This must be done by taking care to preserve the continuity of $T(\vec{r})$ and its first derivative at Γ_p^*. Indeed, the solution scheme actually only requires the ray-representation of $\vec{\mathcal{G}}[T(\vec{r})\vec{C}_p^*(\vec{r})]$, which is dictated by the local behavior at Γ_p^* of the amplitude-modulated FW's. The first- and second-order asymptotic contributions of the modulated FW diffraction at Γ_p^* will be affected by the value of $T(\vec{r})$ and its derivative at Γ_p^*, respectively. This process basically corrects the second-order contribution (and then the ray representation of $\vec{u}_d$) with a slope-diffraction term whose practical expression agrees with the slope-UTD. This issue may be particularly important for low sidelobe arrays that require a pronounced edge tapering.

B. Weak Spatial Aperiodicity of the Array

The concept of the adiabatic modification can be also applied when the array exhibits a weak aperiodicity, i.e., a gradual spatial modification of a geometrical parameter of the basic cell. This parameter, that we denote by $d(\vec{r}_i)$ (being $\vec{r}_i$ the position of the single cell), leads to a local infinite array solution $\vec{u}_{\infty}(\vec{r},\, d(\vec{r}_i))$, which is, for each ith cell, the periodic continuation of the same cell with its local $d(\vec{r}_i)$ parameter. The knowledge of $\vec{u}_{\infty}(\vec{r},\, d(\vec{r}_i))$ requires a parametric solution of the basic cell, which is a numerically complex matter since it requires a MoM matrix inversion for each value of the parameter; however, the construction of the MoM matrix elements may be straightforwardly dependent on the actual parameter, leading to a decrease in the matrix filling time.

Regarding the solution of the fringe IE, the basic array of sources $\vec{C}_p^*(\vec{r})$ in (34) possesses weakly aperiodic contour elements $\vec{c}_p(\vec{r}-\vec{r}_{pi})(\vec{r}_{pi}\in\Gamma_p^*)$. By invoking the locality of the diffraction principle at high frequency, each contribution of the diffracted ray representation of $\vec{\mathcal{G}}[\vec{C}_p^*(\vec{r})]$ and, consequently, of $\vec{u}^d$, has a structure which depends on the local periodicity of the exciting FW's in the neighborhood of the diffraction points [9].

VI. Selection of the Diffracted Rays and Illustrative Examples

In spite of the fact the infinite-array solution $\vec{u}_{\infty}(\vec{r})$ may be sometimes represented in terms of a large number of FW's, we emphasize that as far as the unknown current is concerned the number of FW's producing significant diffracted rays for each edge *is limited to the propagating FW's (often only one) plus only one evanescent FW per edge,* while an accurate representation of the forcing field $\vec{v}^{ext}$ may require one or two diffracted rays more per edge.

To illustrate this aspect, let us consider an array of $N_x \times N_y$ slots fed by uniform amplitude and phase excitation [$k_{xs}=k_{ys}=0$ in (31)]. In our notation, $\vec{v}_{\text{ext}}$ and $\vec{u}_d$ represent for this case magnetic field and magnetic current, respectively. Suppose only one homogeneous FW occurs. This FW [which is denoted by $m=(m_x,\, m_y)=(0,\, 0)$] propagates with vector wavenumber $\vec{k}_{(0,0)}=k\hat{z}$, thus producing for each observation point four diffracted rays orthogonal to each edge of Γ_p^* (see Fig. 3) and four diffracted rays coming from the vertices. Accordingly, four modulating edge-diffracted ray functions $a_{mq}(\vec{r})$ are used for representing the unknown magnetic current via (18), i.e.,

$$a_{(0,0),1}(x,\, y) = \frac{e^{-jk(L_y-y)}}{[(k(L_y-y)]^{3/2}}\,\mathcal{F}_s[(k(L_y-y)] \tag{42}$$

$$a_{(0,0),2}(x,\, y) = \frac{e^{-jk(L_x-x)}}{[(k(L_x-x)]^{3/2}}\,\mathcal{F}_s[(k(L_x-x)] \tag{43}$$

$$a_{(0,0),3}(x,\, y) = \frac{e^{-jk(L_y+y)}}{[(k(L_y+y)]^{3/2}}\,\mathcal{F}_s[(k(L_y+y)] \tag{44}$$

$$a_{(0,0),4}(x,\, y) = \frac{e^{-jk(L_x+x)}}{[(k(L_x+x)]^{3/2}}\,\mathcal{F}_s[(k(L_x+x)] \tag{45}$$

where the origin of the reference system is placed at the center of the array and $2L_x=(N_x+2)\,d_x$ and $2L_y=(N_y+2)\,d_y$. The index in parentheses denotes the exciting FW wavenumber and the indexes 1, 2, 3, and 4 denote the four edges of Γ_p^* starting from that parallel to x with positive y and proceeding clockwise (see Fig. 4).

Significant edge-diffraction contribution due to evanescent FW's are also included to represent the fringe unknowns. The evanescent FW index is different for each of the four edges of $\vec{C}_p^*$. The correspondence between the four edges and the dominant evanescent FW mode index $m=(m_x,\, m_y)$ [see (30) and (31)], is as follows:

$$1\to(0,\,-1),\ 2\to(-1,\,0),\ 3\to(0,\,1),\ 4\to(1,\,0). \tag{46}$$

This association is deduced on the basis of the physical interpretation of the 2-D case of [1, fig. 4 and relevant comments]. The expression of the correspondent FW wavenumbers are

$$\begin{aligned}
\vec{k}_{(0,-1)} &= -\,\hat{y}\,\frac{2\pi}{d_y} + \hat{z}\sqrt{k^2-\left(\frac{2\pi}{d_y}\right)^2}\\
\vec{k}_{(-1,0)} &= -\,\hat{x}\,\frac{2\pi}{d_x} + \hat{z}\sqrt{k^2-\left(\frac{2\pi}{d_x}\right)^2}\\
\vec{k}_{(0,1)} &= \hat{y}\,\frac{2\pi}{d_y} + \hat{z}\sqrt{k^2-\left(\frac{2\pi}{d_y}\right)^2}\\
\vec{k}_{(1,0)} &= \hat{x}\,\frac{2\pi}{d_x} + \hat{z}\sqrt{k^2-\left(\frac{2\pi}{d_x}\right)^2}
\end{aligned} \tag{47}$$

that are each orthogonal to its pertinent edge. Consequently, each evanescent FW produces one diffracted field which prop-

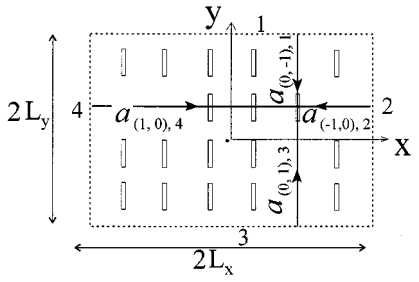

Fig. 3. Diffracted ray basis functions associated to the evanescent TFW's for a slot array with beam in a broadside direction. Each diffracted ray propagates in a direction orthogonal to its pertinent edge.

agates orthogonal to its edge, and additional modulating functions $a_{mq}(\vec{r})$ are used in the expansion of the unknown

$$a_{(0,-1),1}(x,y)=\frac{e^{-jk(L_y-y)}}{\left[\left(k-\frac{2\pi}{d_y}\right)(L_y-y)\right]^{3/2}}\cdot\mathcal{F}_s\left[\left(k-\frac{2\pi}{d_y}\right)(L_y-y)\right] \quad (48)$$

$$a_{(-1,0),2}(x,y)=\frac{e^{-jk(L_x-x)}}{\left[\left(k-\frac{2\pi}{d_x}\right)(L_x-x)\right]^{3/2}}\cdot\mathcal{F}_s\left[\left(k-\frac{2\pi}{d_x}\right)(L_x-x)\right] \quad (49)$$

$$a_{(0,1),3}(x,y)=\frac{e^{-jk(L_y+y)}}{\left[\left(k-\frac{2\pi}{d_y}\right)(L_y+y)\right]^{3/2}}\cdot\mathcal{F}_s\left[\left(k-\frac{2\pi}{d_y}\right)(L_y+y)\right] \quad (50)$$

$$a_{(1,0),4}(x,y)=\frac{e^{-jk(L_x+x)}}{\left[\left(k-\frac{2\pi}{d_x}\right)(L_x+x)\right]^{3/2}}\cdot\mathcal{F}_s\left[\left(k-\frac{2\pi}{d_x}\right)(L_x+x)\right]. \quad (51)$$

Since the diffracted rays are always orthogonal to the edge, no shadow boundary occurs on the array; the presence of vertex diffracted-ray functions is then less important than in the beam scanning case. Nevertheless, we note that the same vertex diffracted rays must be accounted for in the representation of the forcing term of the fringe IE. Eventually, for this case, the solution of the fringe IE requires the inversion of a 8×8 linear system.

The selection of unknowns relevant to this particular example represents a general criterion for broadside beam arrays with linearly polarized elements and does not depend on the element type. For instance, for beamscanning on the plane orthogonal to edges 2 and 4 ($k_{xs} \neq 0$), the edges 1 and 3 are illuminated by skewed FW and the basis functions relevant to edges 1 and 3 must be corrected according to the more general (27). This also creates shadow boundaries on the array aperture thus requiring additional vertex ray compensating terms (note, however, that the number of unknowns is still eight). On the other hand, the diffracted-ray functions at edges 2 and 4 are essentially unaffected by this scan, the only substitution needed being $k-(2\pi/d_x) \rightarrow k-k_{xs}-(2\pi/d_x)$ in (49) and $k-(2\pi/d_x) \rightarrow k+k_{xs}-(2\pi/d_x)$ in (51).

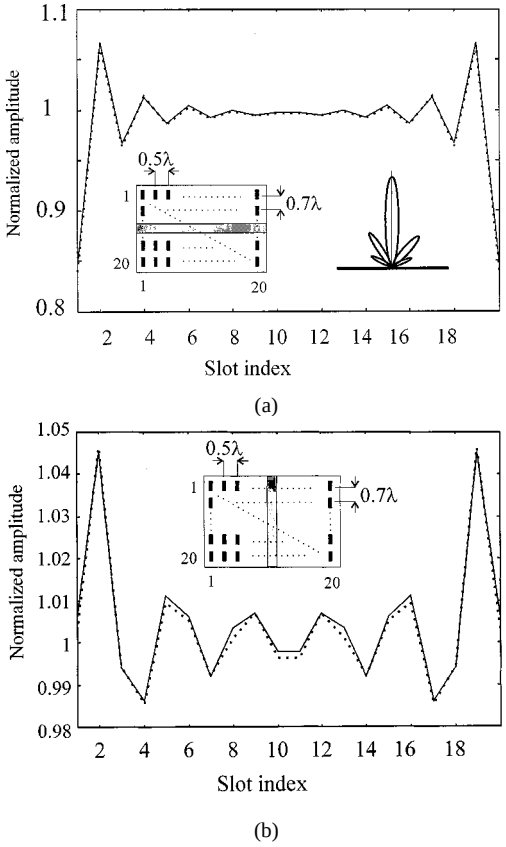

Fig. 4. Normalized amplitude of the magnetic currents versus the slit index for an array of 20×20 slots; $d_x = 0.7\lambda$, $d_y = 0.5\lambda$; $k_{y0} = 0$, $k_{x0} = 0$. Dashed line, element-by-element solution; solid line, TFW-MoM solution. (a) Tenth row. (b) Tenth column.

In the following results, the resonant-slot array is fed by a forcing magnetic field as in [1]. These preliminary results were recently presented in a conference paper [10]. The detailed explanation of the numerical implementation of the reaction integral involved in the MoM-Galerkin formulation with ray-based basis functions is outside the scope of this paper and will be the subject of a future publication. To validate the results, a reference solution has been constructed by means of a conventional element-by-element MoM (dashed line) assuming a single resonant-type basis function on each slot. For the sake of simplicity, our method (continuous line) is applied by choosing the domain A_i of each slot coincident with the subdomain $A_{ip}(P=1)$, and using the function $\vec{c}_p$ equal to the basis function of the element-by-element MoM.

In Figs. 4 and 5, the array is composed by 20×20 y-oriented slots with length 0.5λ and width 0.005λ. The interelement periods are $d_x = 0.5\lambda$ and $d_y = 0.7\lambda$; for the case of Fig. 4 the excitation is uniform in amplitude and phase ($k_{xs} = k_{ys} = 0$)

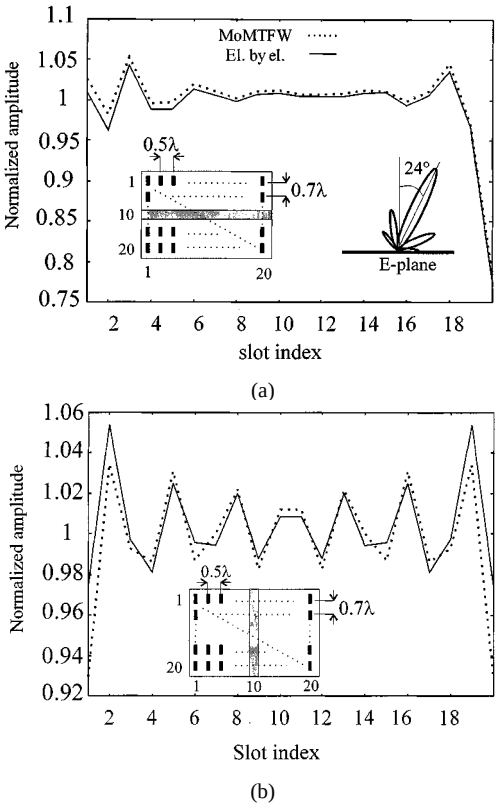

Fig. 5. Normalized amplitude of the magnetic currents versus the slit index for an array of 20 × 20 slots; $d_x = 0.7\lambda$, $d_y = 0.5\lambda$; $k_{x0} = k\sin(24^\circ)$, $k_{y0} = 0$. Dashed line, element-by element solution; solid line, TFW-solution. (a) Tenth row. (b) Tenth column.

and for that of Fig. 5, the excitation is such to give a beam tilt of 18° in the E-plane [$k_{xs} = k\sin(24^\circ)$, $k_{ys} = 0$]. Presented are the normalized magnetic current amplitude versus the slot index, along the central row [Figs. 4 and 5(a)] and the central column [Figs. 4 and 5(b)] of the array. Excellent agreement is observed. We emphasize again that our method implies the solution of an 8 × 8 linear system versus a 400 × 400 linear system relevant to the element-by-element MoM approach.

In Fig. 6, the accuracy and the convergence of the solution are highlighted by observing the errors that are defined as differences between the solution provided by present approach and the reference solution (element-by-element MoM solution). In particular, relative errors per thousands are presented for an array of 20 × 20 slots; $d_x = 0.7\lambda$, $d_y = 0.5\lambda$; $k_{x0} = 0$, $k_{y0} = 0$. The slots labeled by 5, 15, and 20 are affected by a relative error of 5×10^{-3}, 15×10^{-3}, 20×10^{-3}, respectively. Slots without label have a relative error less than 5×10^{-3}. The two pictures differ in the number of rays retained as global basis functions: 1) four diffracted-ray basis functions [only those in (42)–(45)] and 2) eight diffracted-ray basis functions [including those in (48)–(51)]. It is worth noting that the inclusion of the diffracted ray associated with the EFW, which is closer to cutoff, significantly improves the accuracy, while the further introduction of unknowns does not significantly affect the solution. The inclusion of the vertex contribution in the definition of the diffracted ray basis functions implies an error less than 5×10^{-3} everywhere.

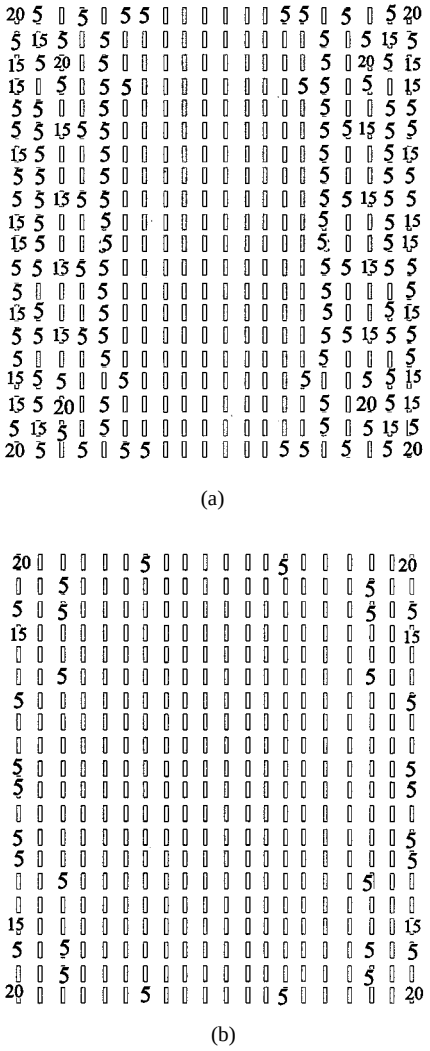

Fig. 6. Relative error per thousands between the element-by-element MoM solution and the TFW solution for an array of 20 × 20 slots; $d_x = 0.7\lambda$, $d_y = 0.5\lambda$; $k_{x0} = 0$, $k_{y0} = 0$. The slots labeled by 5, 15, and 20 are affected by a relative error of 5×10^{-3}, 15×10^{-3}, 20×10^{-3}, respectively. Slots without label have a relative error less than 5×10^{-3}. (a) Four diffracted-ray basis functions [only those in (42)–(45)]. (b) Eight diffracted-ray basis functions [including those in (48)–(51)]. The inclusion of the vertex contribution in the definition of the diffracted-ray basis functions implies an error less then 5×10^{-3} everywhere.

VII. Summary and Discussion

A method has been presented for an efficient full wave solution of large phased arrays. Starting from the solution for the infinite array, a suitable fringe IE has been formulated in which the unknown is the difference between the exact (electric or magnetic) current and that associated with the infinite array. The forcing term of this equation is the (electric or magnetic) field radiated by that part of the ideal infinite array which is complementary to the actual one. After calculating the solution of the infinite array by a conventional scheme, the unknown fringe current is found in three steps. First, moderately small-domain grouping of subdomain functions occupying the same position within each basic cell are collected together, and recognized to form periodic small-element arrays external to the actual domain. Next, the unknown current is represented in terms of collective basis functions that modulate the array-element currents

by special functions with domain on the overall arrays. These modulating functions are shaped like FW-excited diffracted rays at the edges of each external small element array. Finally, a conventional MoM scheme is applied to these entire domain basis functions for solving the IE.

Some considerations of the properties of this approach are summarized herein.

1) In defining the entire domain basis functions, a different set of diffracted rays should be defined for every FW of each small element array. Comparisons with an element-by-element MoM solution have shown that only the diffracted rays corresponding to the homogeneous FW and to one evanescent FW are required for an accurate prediction of the fringe field employed in the ensuing full wave solution. Therefore, the number of entire domain basis functions involved in this full wave analysis of the finite array is remarkably small when compared with an element-by-element approach and almost independent of the global dimension of the array.
2) To represent the forcing term of the IE an asymptotic ray expansion is suggested here, which makes direct use of the active Green's function of the canonical, semi-infinite array and corner array of dipoles weighted by the moment of the basic small-domain element. However, the procedure may be applied as well if one calculates the forcing term by the direct spatial summation of the field contributions from the external elements or, alternatively, from the internal ones, using (6).
3) In the case tested, it is found that our solution works well also at the edge element of the array. This property is motivated by the fact that the rays of the asymptotic expansions arise from edge points that are shifted one period from the edge sources, according to the fact that the forcing term of the IE is associated with the field radiated by the suppressed part of the infinite array. This ensure a quasi-asymptotic structure of the FW diffracted fields even for the edge elements.
4) In defining the diffraction points on rectangular edges under FW excitations, no numerical minimization of distance functions are needed since the position of the diffraction points are defined in analytical form.
5) This method, like all akin methods that employ the infinite-array solution (e.g., [11]) as a starting point to avoid the element-by-element approach, is naturally suited for the analysis of arrays on a periodic lattice with periodic excitation. However, our method can also be applied to the aperiodic case of a smoothly tapered excitation or weakly aperiodic spacing by adiabatically conforming infinite array solutions on the local geometry and tapering and defining the diffracted rays on which to expand the forcing term and the fringe unknown current on the basis of the local edge behavior of the amplitude-modulated FW's.
6) In the analysis of the basic cell, the current is often conveniently represented by a few entire domain functions, usually called "modes," either of conventional or nonconventional kind [12]–[14] and which provide a strong saving in computational time. The support of these modes is not small in terms of wavelengths, and one could object that the definition of the diffracted rays to construct the array basis function is not precise. However, an obvious way out is to represent the entire-domain modes via smaller subdomain functions, and then proceed as above. The number of basis functions needed to represent the current radiation is the number of phase centers and, because of the smoothing property of propagation, this number is much smaller than that required in the analysis of the basic cell, i.e., to determine the detailed shape of the current. This observation also applies to the array-global entire domain basis functions of diffractive nature employed here. This has been shown in the prototypical calculations for the 3-D, resonant slot array discussed above, where only one phase center was enough, i.e., no need was found to break the slot entire domain function into smaller supports to evaluate diffraction. An analysis of a more complex case of array involving rectangular apertures along with quantitative guidelines for the efficient calculation of the MoM matrix elements will be the subject of future publications.

Finally, we remark that the method presented here can also be directly applied to the problem of scattering from periodic finite surfaces such as those occurring in engineering applications involving frequency selective surfaces, polarizers, or grating reflectors.

ACKNOWLEDGMENT

The authors would like to thank M. Biagiotti for providing the numerical results.

REFERENCES

[1] A. Neto, S. Maci, G. Vecchi, and M. Sabbadini, "A truncated floquet wave diffraction method for the full-wave analysis of large phased arrays—Part I: Basic principles and 2-D case," IEEE Trans. Antennas Propagat., vol. 48, Mar. 2000, to be published.
[2] F. Capolino, M. Albani, S. Maci, and L. B. Felsen, "Frequency domain Green's function for a planar periodic semi-infinite phased array—Part I: Truncated Floquet wave formulation," *IEEE Trans. Antennas Propagat.*, vol. 48, pp. 67–74, Jan. 2000.
[3] ——, "Frequency domain Green's function for a planar periodic semi-infinite phased array—Part II: Diffracted wave phenomenology," *IEEE Trans. Antennas Propagat.*, vol. 48, pp. 75–85, Jan. 2000.
[4] F. Capolino, S. Maci, and L. B. Felsen, "Asymptotic high-frequency Green's function for a planar phased sectoral array of dipoles," *Radio Sci.*, vol. 35, no. 2, Mar./Apr. 2000.
[5] S. Maci, M. Albani, and F. Capolino, "ITD formulation for the currents on a plane angular sector," *IEEE Trans. Antennas Propagat.*, vol. 46, pp. 1318–1327, Sept. 1998.
[6] L. Carin, L. B. Felsen, and T.-T. Hsu, "High-frequency fields excited by truncated arrays of nonuniformly distibuted filamentary scatterers on an infinite dielectric grounded slab: Parameterizing leaky mode-Floquet mode interaction," *IEEE Trans. Antennas Propagat.*, vol. 44, pp. 1–11, Jan. 1996.
[7] L. Borselli, S. Maci, A. Toccafondi, and M. Grassi, "High-frequency description of truncated Floquet-waves and guided-waves for a semi-infinite array of line sources on a grounded dielectric slab," in *Conf. Antennas Propagat. Soc.*, Montreal, Canada, July 1997.
[8] S. Maci, L. Borselli, and L. Rossi, "Diffraction at edge of a truncated, grounded dielectric slabs," *IEEE Trans. Antennas Propagat.*, vol. 44, pp. 863–873, June 1996.
[9] L. B. Felsen and E. G. Ribas, "Ray theory for scattering by two dimensional quasi-periodic plane finite arrays," *IEEE Trans. Antennas Propagat.*, vol. 44, pp. 375–382, Mar. 1996.

[10] A. Neto, S. Maci, G. Vecchi, and M. Biagiotti, "Full-wave analysis of a large rectangular array of slots," in *Conf. Antennas Propagat. Symp.*, Atlanta, GA, June 1998.
[11] A. Skrivervik and J. Mosig, "Finite planed array of microstrip patch antennas: The infinite array approach," *IEEE Trans. Antennas Propagat.*, vol. 40, pp. 579–582, May 1992.
[12] G. Vecchi, P. Pirinoli, L. Matekovits, and M. Orefice, "Application of numerical regularization options to the integral-equation analysis of printed antennas," *IEEE Trans. Antennas Propagat.*, vol. 45, pp. 570–572, Mar. 1997.
[13] ——, "Static, attachment, and resonant modes in the analysis of printed antennas of arbitrary shape," in *Proc. Int. Conf. Electromagn. Adv. Applicat. 1997*, Torino, Italy, Sept. 1997, pp. 329–332.
[14] ——, "A numerical regularization of the EFIE for three-dimensional planar structures in layered media," Int. J. Microwave Millimeter-Wave Computer-Aided Eng., pp. 410–431, Nov. 1997, to be published.

Stefano Maci (M'92–SM'99) was born in Rome, Italy, in 1961. He received his Doctor degree in electronic engineering from the University of Florence, Italy, in 1987.

In 1990, he joined the Department of Electronic Engineering, University of Florence, Italy, as an Assistant Professor. In 1998 he was appointed Associate Professor of Electromagnetism at the University of Siena, Italy. In 1997 he was an invited Professor at the Technical University of Denmark, Copenhagen. Since 1996 he has been involved in projects of the European Space Agency, Noordwijk, The Netherlands, regarding the electromagnetic modeling of antennas. His research interests are focused on electromagnetic theory, mainly concerning high-frequency methods for electromagnetic scattering and diffraction. He also developed research activity on microwave antennas, particularly focused on the analysis, synthesis, and design of patch antennas.

Dr. Maci received the national Young Scientists "Francini" award for the Laurea thesis in 1988 and the "Barzilai" prize for the best paper at the National Italian Congress of Electromagnetism (XI RiNEm) in 1996. He is an Associate Editor of the IEEE TRANSACTIONS ON ELECTROMAGNETIC COMPATABILITY.

Giuseppe Vecchi (M'90) received the Laurea and Ph.D. degrees in electronic engineering from Politecnico di Torino, Torino, Italy, in 1985 and 1989, respectively.

From August 1989 to February 1990, he was a Visiting Scientist at Polytechnic University, Farmingdale, NY, through an Italian National Research Council (CNR) Fellowship. He then joined the Politecnico di Torino as a Researcher in the Department of Electronics. In November 1992, he was appointed Associate Professor of electromagnetism. His main research activities concern analytical and numerical techniques in high- and low-frequency electromagnetics, electromagnetic compatibility, and fractal electrodynamics.

Andrea Neto was born in Naples, Italy, in 1968. He received the Laurea degree (*cum laude*) in electronic engineering from the University of Florence, Italy, in 1994.

In 1995, he spent one year of research as Young Graduate Trainee at the European Space Agency (ESTEC-ESA), Noordwijk, The Netherlands. Since 1996, he has been involved with a Ph.D. research program at the University of Siena, Italy, concerning methods for the analysis of large arrays. He is currently with the Antenna Section of ESTEC-ESA. His research is focused on high frequency and numerical methods in electromagnetics.

Marco Sabbadini received the Laurea degree in electronic engineering from the University of Rome La Sapienza, in 1983.

From 1983 to 1988, he was with the Antenna Department, Alenia Aerospazio, Rome, Italy. In August 1988 he joined the European Space Agency as Antenna Engineer in the Electrical System Department, European Space Research and Technology Center, Noordwijk, The Netherlands. His main fields of activity are the development of space antenna technology, with special stress on array antennas, electromagnetic modeling techniques, and tools for antenna design.